

PROCESSING AND CHARACTERIZATION OF SiC FIBER REINFORCED Ti-15V-3Cr MATRIX COMPOSITES

Y.W. Xun, M.J. Tan

School of Mechanical and Production Engineering, Nanyang Technological University
Singapore 639798

SUMMARY: SiC/Ti-15V-3Cr metal matrix composites have been developed using the hot uniaxial pressing of an assembly of Ti-15V-3Cr foils stacked between uniaxial fiber mats. The interfacial microstructures and interfacial reaction kinetics were analyzed with respect to the reactives of the interface and the relevant elements involved. The recrystallization of matrix materials played a great role in refining the matrix grain size, improving the diffusion bonding of matrix/matrix interface as well as fiber/matrix interface. A layer of chemical reaction products mainly consisting of titanium carbides was observed at the fiber/matrix interfaces. Limited reactions were observed compared with those that occurred in the SiC/Ti-6Al-4V system due to a lower processing temperature. This advantage was attributed to the temperature dependence of reaction driving-force. Three types of reaction mechanisms were suggested based on the controlling kinetics of reaction rate.

KEYWORDS: titanium matrix composites, consolidation, C-coated SiC fiber, Ti-15V-3Cr alloy, superplastic flow, diffusion bonding, interfacial reaction, reaction rate

INTRODUCTION

Titanium matrix composites (TMCs) have been under development for many years due primarily to the high specific strength offered by Ti alloys and the persistent drive from industry for improved high-temperature materials. The incorporation of SiC fibers in TMCs has led to the development of high strength, low density and high creep resistance properties. These composites have applications in the aerospace industry as structural materials for aerojet components and compressor blades.

Several techniques have been developed to TMCs with long fiber reinforcements, such as powder-cloth processing, foil-fiber-foil processing [1-2], etc. These processes usually involve a consolidation stage using diffusion bonding or hot isostatic pressing where the consolidation temperatures are in excess of 800°C for a significant period of time. C-coated SiC fibers tend to react with the matrices under these conditions, leading to the formation of a brittle reaction layer and deterioration of the mechanical properties of the composites [3-5]. The interfacial reaction can be controlled by (1) lowering the bonding

temperature, at the expense of a high bonding pressure and/or a long bonding time; and (2) using protective coatings such as C/TiB₂ and C/TiC/Ti, to improve the performance of the reinforcement; and (3) adding alloying elements such Nb, Al, Cr, V, Sn, Zr, Mo to titanium matrix to produce less reactive matrices (e.g. Ti-6Al-4V, Ti-13Cr-11V-3Al, Ti-1100, Ti3Al-20Nb, Ti-15Mo) [6-8].

Most of the current work in TMCs is directed towards the Ti-6Al-4V alloy because it is most readily available and familiar to most users. Several studies have been aimed at determining the pore-closing kinetics, the interfacial reaction kinetics, the alloying element effects, and the influence of functionally graded coatings on SiC fibers [9-10]. Despite the popularity of the SiC/Ti-6Al-4V system, there are clear advantages in considering the β or β -metastable alloys as matrix alloys. They offer greatly improved formability and hence lower material costs in terms of producing the thin foils used in diffusion bonding. Also, lower consolidation temperature can be used, leading to a reduction in the thickness of the unavoidable reaction layer.

The β -metastable Ti alloy Ti-15V-3Cr-3Sn-3Al matrix was selected for investigation in this paper. The studies involved the diffusion bonding of alternate layers of aligned SiC fibers and Ti-15V-3Cr-3Sn-3Al matrix foils at elevated temperatures under pressure. The composite was characterized to ensure 1) minimized interfacial reactions; 2) complete closure of interfacial voids; 3) the desired matrix microstructure; 4) the desired mechanical properties; 5) minimized fiber damages; 6) a uniform fiber distribution. All these are necessary for successfully setting up a novel TMC system.

EXPERIMENT

The matrix material used for this investigation was β -metastable Ti-15V-3Cr-3Sn-3Al (Ti-15V-3Cr) alloy in the form of cold-rolled foils of 100 μm thickness. Its compositions are given in Table 1, along with its β -transus temperature measured by differential thermal analysis. The material has two main phases, namely body-centered cubic β phase and hexagonal close-packed α phase. The volume fraction of the latter is less than 10%. This alloy can be heat-treated to high strength levels up to 1180 MPa [11-13], higher than the industry standard Ti-6Al-4V alloy. Also, this alloy can be readily processed into thin foil through a commercial production process. The most important advantage of this alloy is its excellent low-temperature formability. The studies on the superplastic forming properties of Ti-15V-3Cr sheets reveal that the elongation can reach 500% at 700°C at strain rate of $1 \times 10^{-4} \text{ s}^{-1}$, making matrix flow possible during consolidation.

Table 1. Composition and mechanical properties of 0.1 mm Ti-15V-3Cr foils

Composition (wt%)								β transus	σ_b	E	δ
V	Cr	Al	Sn	Fe	Si	O	Ti	temperature (°C)	(MPa)	(GPa)	(%)
15.2	3.1	3.1	2.9	0.2	0.024	0.14	balance	760	784	77.3	11

Composite reinforcement was in the form of SiC fibers 120 μm in diameter with commercial label GB-C. These fibers have a tungsten core and a carbide coating of about 2.5 μm thick. The properties of these fibers are listed in Table 2, and compared with the properties of the SCS-6 fibers produced by Textron Speciality Materials. Although the

current fiber is inferior to SCS-6 fiber from the viewpoint of the listed properties in Table 2, it is sufficient to meet the requirements of current research.

Table 2. Comparison of GB-C SiC fibers with commercial SCS-6 fibers

Reinforcement	σ_b (MPa)	E (GPa)	Coating thickness (μm)	Coating method	Density (g/cm^3)	Diameter (μm)
GB-C	2700	400	2.5	Single-layer	3.44	120
SCS-6	3450	481	3	Graded-layer	3.05	142

The fiber were wound into a mat with a spacing of 180 to 240 μm and held by an acrylic binder. Composites were produced by bonding alternately stacked fiber-mats and matrix-foils using a vacuum hot-press. The stacking configuration had a triangular array of unidirectional fibers (Figure 1) in the cross section. A fully consolidated composite was designed to have a fiber volume fraction of about 15% to 23%.

The hot-pressing temperatures were 750°C, 820°C and 880°C. For grain size control during processing, a consolidation temperature lower than β -transus (760°C) is best. The temperature of 820°C and 880°C were used for comparison. The consolidated samples were furnace cooled at a rate of 0.14 $^{\circ}\text{C}/\text{s}$ after fabrication. Some samples were exposed to high temperatures for up to 9 h in order to investigate interface stability and reaction kinetics. Microstructural specimens were cut perpendicular to the fiber axial direction for microstructural examinations and sample preparation followed standard procedures of lapping, polishing and etching.

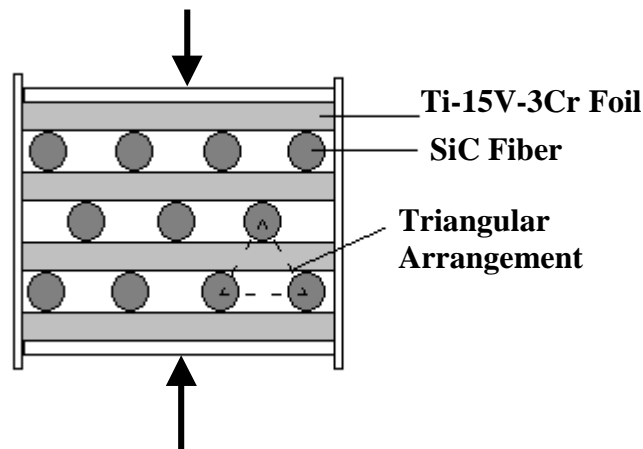


Figure 1. Schematic illustration of the assembly with triangular array configuration

RESULTS AND DISCUSSION

Microstructures

A cross-section of one of the composite samples is present in Figure 2 to illustrate the overall morphology of the material. The sample was consolidated at 750°C under 80 MPa for 2 h and was further exposed at the same temperature for 4 h (total exposure of 6 h). Full consolidation was achieved under the experimental conditions. The observations also reveal that the fiber distribution is uniform.

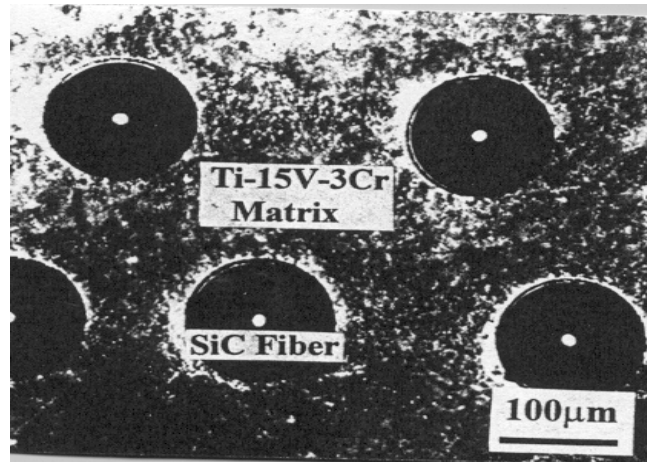


Figure 2. Cross-section of a SiC/Ti-15V-3Cr composite consolidated at 750°C under 80MPa for 2 h and further exposed at the same temperature for 4 h

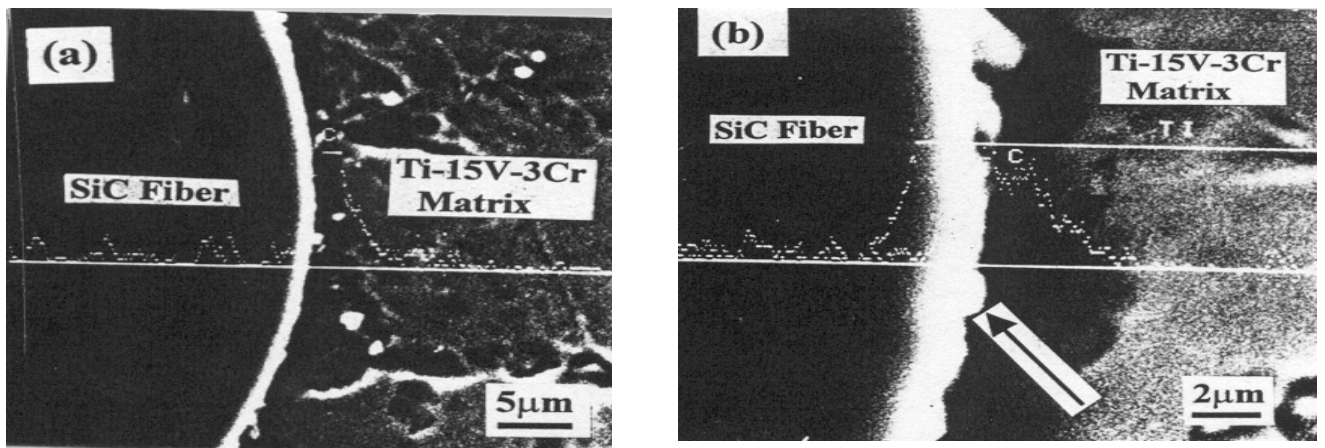


Figure 3. Interface microstructure between the C-coated SiC fiber and Ti-15V-3Cr matrix after exposure a) at 750°C for 9 h; b) 880°C for 3 h, superimposed with C element analysis

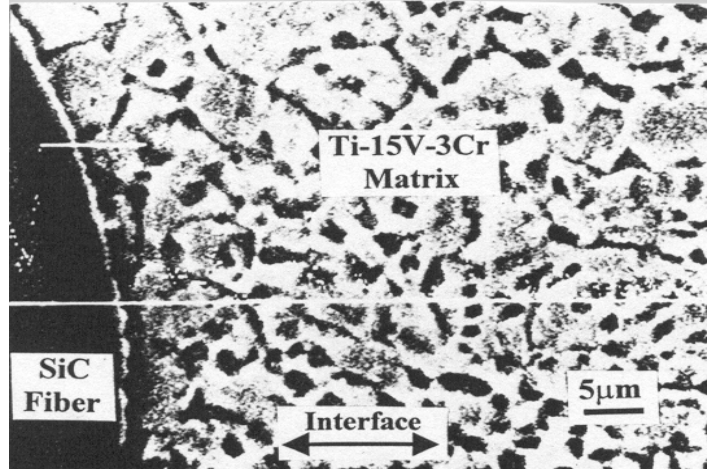


Figure 4. Matrix/matrix interface microstructure of the composite consolidated at 750°C under 80 MPa for 2 h, superimposed with C elemental analysis

A series of samples were manufactured under different conditions for the comparison of interface stability and reaction kinetics. Representative interfacial microstructures are shown in Figure 3 (a) and (b). Figure 3 (a) depicts the reaction layer developed at SiC/Ti-15V-3Cr interface. The sample was processed at 750°C with a total thermal-exposure of 9 h with the processing pressure of 80 MPa having been applied for the initial 3 h. Figure 3 (b) illustrates the interfacial structure of the sample pressed at 880°C under pressure 80 MPa for 3 h. Both exhibit a layer of reaction products of essentially similar morphology. There are no defects in the interfaces between the reaction layer and either the fiber or matrix, indicating sound bonding. It has been shown that the growth of the reaction layer in SCS/Ti-6Al-4V and unalloyed titanium is more rapid adjacent to the β -grains than in the α -phase [14-15]. But the observations based on Figure 4 are not the case. This can be attributed to the fact that the reaction rate has been decelerated by the presence of alloying elements, particularly those that stabilize the β -phase, such as V and Cr.

The microstructure of the matrix/matrix interface consolidated at 750°C under 80 MPa for 2 h is shown in Figure 4. The solid-state bond created between two matrix foils was so well formed that it was impossible to detect the original interface, even at high magnification. At superplastic temperature (typically $>0.75T_m$, where T_m is the absolute melting point of the material), the matrix foil-foil interfacial diffusion processes, and particularly grain-boundary diffusion, usually are rapid, permitting extensive boundary migration and void shrinkage occurring at interfaces. The grain-boundary diffusivity, D_b , can be expressed by [16]:

$$D_b = 1.0 \times 10^{-4} \exp\left(-9.35 \frac{T_m}{T}\right) m^2 s^{-1} \quad (1)$$

for $1.0 < T_m/T < 2.4$, where T_m is the absolute melting point of the materials. At $T = 0.75 T_m$, the value of D_b is estimated to be about $4 \times 10^{-10} \text{ m}^2 \text{ s}^{-1}$; i.e., atoms diffuse about $10 \mu\text{m s}^{-1}$.

Figure 4 also reveals the changes in matrix microstructure during consolidation. In the region of the bonding interface, the average grain size is $5 \mu\text{m}$; in the region of the foil-center the grain size is about $10 \mu\text{m}$. This fine-grained structure can be attributed to the fact that the matrix materials were treated by prior quenching from the β region (solution

treatment) followed by cold working. After such a treatment, subsequent high temperature consolidation will facilitate recrystallization and provide for a microcrystalline structure. During consolidation, the materials near the foil-foil interfaces will undergo large-scale deformation (plastic flow), driving significant dynamic recrystallization in this region. While the foil-center regions will undergo relatively small-scale deformation and the fine-grained structure in this region can be considered to be the result of a static recrystallization process. In a general case, the critical size of the newly formed grains D_{cr} can be defined as [17]

$$D_{cr} = \frac{4r}{3f} \quad (2)$$

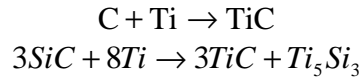
where f is volume fraction of new-phase particle and r is the particle radius. The transition from the impeding of recrystallization by small particles to its acceleration by coarse precipitates is mainly related to the parameter f/r . Hot or cold preworking is usually necessary for subsequent recrystallization because the value of f can be greatly increased by prestraining [18]. In present case, the cold working of Ti-15V-3Cr matrix prior to consolidation played a critical role in structure refining.

These microstructure changes are important for consolidation [19-20]. The presence of many grain boundaries in fine-grained matrices provides short-circuit paths for diffusion. Grain-boundary migration is also faster in fine-grained than in coarse-grained matrices. The creep rate of the former matrix is faster than the latter. Also, the low-temperature formability can be improved: Ti-15V-3Cr alloy with a coarse-grained microstructure is capable of exhibiting the superplastic effect in the β -region only, whereas under present conditions, the alloy shows high ductility and low flow stress in the $\alpha+\beta$ region.

Energy-dispersion spectroscopy and linescan analyses showed that the reaction layer contained principally Ti and C. It indicated that the layer mainly consisted of titanium carbide and that insignificant amounts of Ti_5Si_3 formed during processing. The C-coating layer was designed to protect the fiber from surface damage, arising either from mechanical or chemical effects, but the layer itself requires protection because it can be consumed by chemical reactions. One method of providing this protection is by deposition of a layer of TiC over the C-coating [21-24]. If the C-coating is fully consumed at elevated temperatures, Si from SiC will diffuse into TiC to form Ti-Si-C compounds. If parts of the coating at a region of the sample has been locally consumed and parts remains intact, it can be suggested that the nature of the reaction layer altered as the C-coating was consumed and the silicon carbide was exposed.

Fiber/matrix Interface Stability

The thermochemical compatibility of the fiber/matrix interface is of primary concern in fiber-reinforced metal matrix composites. A thermochemically compatible interface should either be in thermodynamic equilibrium or be kinetically sluggish, i.e., thermal dynamic equilibrium, or the driving force is too small to cause any significant reaction over a prolonged period of operation at service temperatures. Interface stability in a multicomponent system is controlled by a number of chemical, thermodynamic and kinetic factors. Reaction of C and SiC with the Ti-based matrix is thermodynamically favored under present consolidation conditions:



For TiC, the standard enthalpy and Gibbs free energy of formation at 298°K are $\Delta H_{f,298}^\circ = -183.7 \text{ KJmol}^{-1}$ and $\Delta G_{f,298}^\circ = -179 \text{ KJmol}^{-1}$. Because some heat capacities are unavailable, It is not possible to calculate ΔG° and K for the above reactions at consolidation temperatures. Literature has shown that the values of ΔG° at 950°C for above reactions are -170 KJ mol^{-1} and -189 KJ mol^{-1} [25], respectively. At present consolidation temperature, 750°C, the ΔG° value should be much less than that at 950°C. This means there is less reaction driving force for SiC/Ti-15V-3Cr system compared with SiC/Ti-6Al-4V system which needs a higher consolidation temperature.

Reaction Kinetics

Three mechanisms can be used to describe the reaction process. They are reaction-controlled process, diffusion-controlled process, and rate-controlled process. For a displacement reaction couple (as shown in Figure 5), it is generally anticipated that the chemical reaction first takes place between the atoms in the surface layers, driven by the reduction in Gibbs free energy. At this early stage the reaction products form a thin layer so that the supply of the required atoms for the reaction can be finished through diffusion around and across the interface. So the reaction can continue at its own “pace”, i.e., the rate of the reaction is reaction-controlled. Because the reaction rate remain unchanged during the course of reaction, the kinetics can be expressed by the equation

$$x = k_{rac} \cdot t \quad (3)$$

where x is the thickness of the reaction layer, t is the reaction time and k_{rac} is the reaction constant.

The second mechanism begins to work as the reaction layer gets thicker and thicker. The diffusivities of relevant atoms in the reaction layer become dominant factors for reaction “pace” because they determine the efficiency of atom supply. So this process is named diffusion-controlled reaction and characterized by the following equation

$$x = k_{dif} \cdot \sqrt{t} + x_0 \quad (4)$$

where k_{dif} is a rate constant, t is the time and x_0 is the x value at $t = 0$. The values of x_0 and k_{dif} can be calculated if sufficient experimental data are available.

The diffusion-bonded samples were subjected to isothermal exposure treatment, and then they were sectioned, mounted and polished for metallographic examination in the scanning electron microscope. The thickness of the reaction layer was measured at more than 30 separate locations for each sample. Changes in thickness of the reaction layer are shown in Figure 6. The data points for each treatment temperature were fitted with a straight line to estimate a generalized reaction rate constant. The fitted equations were

$$x = 0.0352\sqrt{t} + 0.0249 \quad \text{at } 780^{\circ}\text{C} \quad (5)$$

$$x = 0.0533\sqrt{t} - 0.0733 \quad \text{at } 820^{\circ}\text{C} \quad (6)$$

$$x = 0.0641\sqrt{t} + 0.1142 \quad \text{at } 880^{\circ}\text{C} \quad (7)$$

where the thickness is presented in microns and the time in minutes. Based on the results from reference [14], the reaction layer thickness between super- α_2 and the C-coated SCS fiber at 982°C can be fitted to the following function for comparison (assuming the reaction mechanisms for two systems is similar)

$$x = 0.085\sqrt{t} + 0.149 \quad \text{at } 982^{\circ}\text{C} \quad (8)$$

These equations provide quantitative descriptions for the diffusion-controlled reactions and from which the reaction results at a specific time can be calculated. Moreover, the fact that the k_{dif} value increases with the increase of reaction temperatures reveals the importance and advantage of using matrix materials with low consolidation temperature.

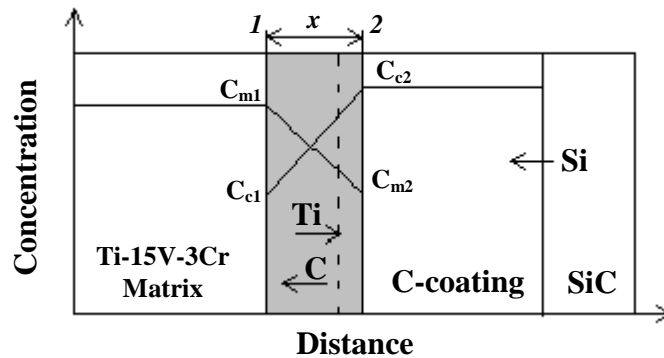


Figure 5. Schematic illustration of the geometric relationships in a displacement reaction couple and the change in concentrations (the shaded area depicts interfacial reaction layer and the dotted line depicts the original interface from which it can be seen that the phase growth is mainly towards the matrix)

The third mechanism is, strictly speaking, a special case of diffusion-controlled kinetics. For a given reaction the diffusivities of reactants are usually quite different in the reaction layer. When the difference is great enough to effect the supply rate of atoms and the reaction rate, the reaction rate is considered to be controlled by the faster diffusing reactant, i.e., the reaction “pace” is mainly related to the highest diffusivity value for all reactants. There is a lack of information on the diffusivities of many elements in certain mediums, so it is difficult to quantify the rate-controlled reaction. But if it has been known that one diffusivity is several orders faster than the others in a chemical reaction, some relatively certain conclusions can be drawn based on this mechanism and Equation 4.

Assuming the present reaction $\text{Ti} + \text{C} \rightarrow \text{TiC}$ is a pseudo-binary couple, consisting of a matrix reactant and a coating reactant, and the concentrations of the reactions are in a steady state, in most cases, the diffusion-controlled kinetics are determined by the diffusivities of the relevant elements across the reaction layer and the concentrations of the elements at the interfaces.

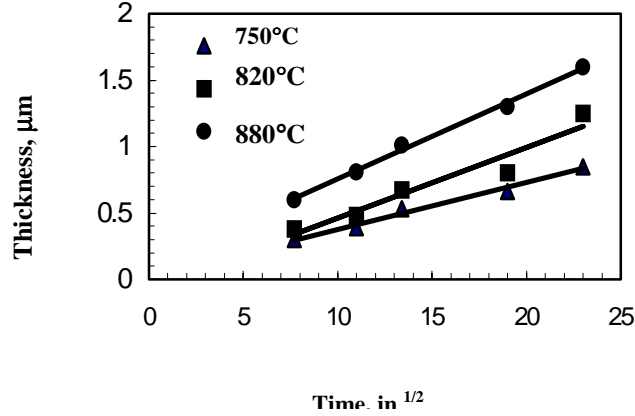


Figure 6. Thickness variation of the interface reaction layer between the C-coated SiC fiber and the Ti-15V-3Cr matrix as a function of the square root of the exposure time at different temperatures (the experimental results are shown as data points, and the straight lines are the least-square fits to the points)

The thickness of the reaction layer can be directly related to the diffusivities of the reactants through the reaction layer [26].

$$x^2 = 2 \left(D_m \frac{C_{m1} - C_{m2}}{C_{m2}} + D_c \frac{C_{c2} - C_{c1}}{C_{c1}} \right) \cdot t \quad (9)$$

where D and C are diffusivity and concentration, respectively; subscripts m and c designate the matrix and the fiber coating; and subscripts 1 and 2 refer to the matrix/compound interface and the coating/compound interface. Comparing Equation 4 and Equation 9, we have

$$k_{dif}^2 = 2 \left(D_m \frac{C_{m1} - C_{m2}}{C_{m2}} + D_c \frac{C_{c2} - C_{c1}}{C_{c1}} \right) \quad (10)$$

Assume $C_{m1}=0.8$ (Ti in Ti-15V-3Cr matrix), $C_{m2}=0.5$ (Ti in TiC), $C_{c1}=1$ (C in C-coating), and $C_{c2}=0.5$ (C in TiC). Substituting these values into Equation 10, we obtain

$$0.6D_m + D_c = \frac{1}{2}k_{dif}^2 \quad (11)$$

From references [27-28] we know that diffusivity of C in TiC (D_c) is around 10^{-14} to 10^{-16} m^2s^{-1} , while the diffusivity of Ti in those compounds (D_m) is in the order of 10^{-21} to 10^{-24} m^2s^{-1} . The implication is that the diffusion of C through the reaction layer is the rate-controlling process. Because D_m is at least five orders slower, we can ignore it in Equation 11. Thus we get

$$D_c = \frac{1}{2} k_{dif}^2 \quad (12)$$

Substituting k_{dif} values from Equations 5, 6 and 7 into Equation 12, we get $D_c = 1.97 \times 10^{-17} \text{ m}^2 \text{ s}^{-1}$ at 750°C , $D_c = 2.36 \times 10^{-17} \text{ m}^2 \text{ s}^{-1}$ at 820°C , and $D_c = 3.42 \times 10^{-17} \text{ m}^2 \text{ s}^{-1}$ at 880°C . For comparison, we use the k_{dif} value in Equation 8 and get $D_c = 6.1 \times 10^{-17} \text{ m}^2 \text{ s}^{-1}$ at 982°C (in this case, $C_{ml} = 0.75$ for Ti in Ti_3Al). These results indicate that the diffusivity of C in TiC reaction layer at 982°C is two times higher than that at 750°C .

Generally speaking, the above mechanisms can be of similar importance. But for the sake of convenience or because of the lack of sufficient data points, diffusion-controlled kinetic function is normally used to analysis the experimental data and depict the reaction progress. Reaction -controlled mechanism governs the early stages of reaction and is the key step of determining interfacial stability. Rate-controlled mechanism is a slower one, but it is the only one that can be supported by interfacial morphology. From Figure 3, it can be observed that the interface between C-coating and matrix alloy appears irregular with peaks orientated towards the matrix (depicted by the arrow). Because reactant C has higher diffusivity in TiC than reactant Ti, the reaction is mainly through the diffusion of C across the reaction layer. As C atoms reach the matrix side, they react with the matrix atoms and which make the interface grow into the matrix.

CONCLUSIONS

The SiC/Ti-15v-3Cr system demonstrated itself an attractive system for manufacturing metal matrix composites. Full consolidation and sound bonding were achieved at relatively low processing temperature (750°C). Only limited reaction products were observed between the C-coated fiber and the matrix. The diffusivity of C atoms through reaction layer was the controlling factor that governed the reaction rate as well as the growth kinetics of the reaction layer. The diffusivity of C in TiC compounds was estimated to be $1.97 \times 10^{-17} \text{ m}^2 \text{ s}^{-1}$ at 750°C , only one-third of the diffusivity at 982°C . The recrystallization occurring during high temperature deformation refined the grain size to $5\sim 10 \mu\text{m}$. The observation and calculation results revealed that SiC/ Ti-15V-3Cr system has a good interface stability compared with conventional SiC/Ti-6Al-4V system.

REFERENCES

- [1] R.A. Mackay, P.K. Brindley, F.H. Froes, J. Met., 43 (5) (1991) 23-29.
- [2] S.L. Semiatin, R.L. Goetz, Mater. Res. Soc. Symp. Proc., 273 (1992) 351-364.
- [3] S.F. Baumann, P.R. Brindley, S.D. Smith, Metall. Trans. A, 21A, (1990) 1559.
- [4] J.M. Yang, S.M. Jeng, Scripta Metal., 23, (1989) 1559.
- [5] P.R. Brindley, P.A. Bartolotta, S.J. Klima, NASA Report No. TM-100956, 1988.
- [6] P. Martineau, R. Pailler, M. Lahaye, R. Naslain, J. Mater. Sci., 19, (1984) 2749.
- [7] D.B. Gundel, F.E. Wawner, Scripta Metallurgica et Materialia, 25, (1991) 437.
- [8] M. Nathan, I.S. Ahearn, Mater. Sci. & Eng., A126, (1990) 225.
- [9] A.D. Hill, E.R. Wallach, Acta Metall. Mater., 37, (1989) 2425.
- [10] D.M. Elzey, H.N.G. Wadley, Acta Metall. Mater. 41, (1993) 2297.
- [11] T. Inaba, K. Ameyama, M. Tokizane, ISIJ Int. 31 (8) (1991) 792-798.
- [12] N. Niwa, A. Arai, H. Takatori, K. Ito, ISIJ Int. 31 (8) (1991) 856-862.

- [13] M. Okada, *ISIJ Int.* 31 (8) (1991) 834-839.
- [14] Z.X. Guo, B. Derby, *Composites*, 25, (1994) 630.
- [15] I.W. Hall, J.L. Lirn, J. Rizza, *J. Mater. Sci. Lett.*, 10, (1991) 263-266.
- [16] J.C.M. Hwang R.W. Balluffi, *Sci. Metall.*, 12, (1978) 709-714.
- [17] F.G. Humphreys, *Met. Sci.*, 13, (1979) 136-145.
- [18] F.H. Froes, C.H. Yolton, J.C. Cheshutt, C.H. Hamilton, *Forging and Properties of Aerospace Materials*, The Metals Society, London, 1978, 371-398.
- [19] O.D. Sherby, J. Wadsworth, R.D. Caligiuri, L.E. Eiselstein, B.C. Snyder, R.T. Whalen, *Scr. Metall.*, 13, (1979) 941-946.
- [20] W. Hu, D. Ponge, G. Gottstein, *Mater. Sci Eng.*, A190, (1995) 223-229.
- [21] K.L. Choy, B. Derby, *J. Materials and Manufacturing Processes*, 9[5], (1994) 885.
- [22] K.L. Choy, B. Derby, *J. Microscopy*, 169[2], (1993) 289.
- [23] K.L. Choy, B. Derby, *J. Mater. Sci.*, 29, (1994) 3774.
- [24] K.L. Choy, J. Durodola, B. Derby, C. Ruiz, *Composites*, 26, (1995) 91.
- [25] D.R. Schuyler, M.M. Sohi, R. Mahapatra, in: *Interfaces in Metal-Cermics Composites*, R.Y. Lin, R.J. Arsenault, G.P. Martins, S.G. Fishman (eds.), TMS, Warrendale PA, (1989) 475.
- [26] V.I. Dybkov, *J. Mater. Sci.*, 21, (1986) 3078.
- [27] H.J. Frost, *Deformation Mechanism Maps*, Pergamon, Oxford, 1982, p. 80.
- [28] M. Backhaus-Ricoult, *Metal-Ceramic Interfaces*, M. Ruhle, A.G. Evans, M.F. Ashby and J.P. Hirth (eds.), Pergamon, Oxford, 1990, p. 79.